


RESEARCH ARTICLE

Experimental and model-based investigation of the droplet size distribution during the mixing process in a batch-settling cell

Stepan Sibirtsev  | Lukas Thiel | Song Zhai | Yutang Toni Cai |
Louis Recke | Andreas Jupke

Fluid Process Engineering (AVT.FVT),
RWTH Aachen University, Aachen,
Germany

Correspondence

Andreas Jupke, Fluid Process Engineering
(AVT.FVT), RWTH Aachen University,
Forckenbeckstrasse 51, 52074 Aachen,
Germany.
Email: andreas.jupke@avt.rwth-aachen.de

Funding information

Deutsche Forschungsgemeinschaft,
Grant/Award Number: 466656378

Abstract

The design of a liquid–liquid gravity settler relies on the experimental investigation and model-based description of the phase separation process in a batch-settling cell. However, according to the current state of the art, the modelling assumes a monodisperse droplet size distribution (DSD), which can lead to an inaccurate settler design. This study considers the polydispersity of the initial DSD resulting from the mixing process in the settling cell to enhance the model accuracy. DSDs of o/w and w/o dispersions during the mixing process in a settling cell are investigated in this work for 2-methyltetrahydrofuran/water and decane/water material systems at hold-ups of 25–50 vol.% and stirrer speeds of 400–850 min^{−1}. Sauter mean diameters (SMD) and DSD shapes are analyzed to identify the influence of the investigated parameters on the SMD and DSD and to model the SMD and DSD. The experimental investigation shows that stirrer speed, hold-up, and interfacial tension significantly affect the DSD, while the viscosity of the continuous phase plays a minor role. The SMD is correlated to the Weber number, viscosity group, and hold-up by a model with a mean absolute percentage error (MAPE) of 3.6%. The DSD is described by a log-normal distribution function with a MAPE of 5%. The SMD and DSD models presented in this work can be used to describe the initial DSD of the phase separation process in a batch-settling cell, considering polydispersity and thus increasing the modelling accuracy of the phase separation process.

KEYWORDS

batch-settling cell, droplet size distribution, liquid–liquid dispersion, Sauter mean diameter, Weber number correlation

Abbreviations: 2-MTHF, 2-methyltetrahydrofuran; CDF, cumulative distribution function; DSD, droplet size distribution; MAPE, mean absolute percentage error; SMD, Sauter mean diameter.

Stepan Sibirtsev and Lukas Thiel contributed equally to this study.

This is an open access article under the terms of the [Creative Commons Attribution-NonCommercial](https://creativecommons.org/licenses/by-nc/4.0/) License, which permits use, distribution and reproduction in any medium, provided the original work is properly cited and is not used for commercial purposes.

© 2024 The Author(s). *The Canadian Journal of Chemical Engineering* published by Wiley Periodicals LLC on behalf of Canadian Society for Chemical Engineering.

1 | INTRODUCTION

The separation of liquid–liquid dispersions in gravity settlers is essential in several technical applications of process engineering, for example, liquid–liquid extraction.^[1] The design of a settler can be performed by an experiment and model-based method developed by Henschke.^[2,3] This method first examines the phase separation behaviour in a standardized batch-settling cell at a laboratory scale. The batch-settling cell is a stirred vessel standardized in the sense that its geometric parameters are firmly defined, which makes it possible to compare the experimental data from several authors.^[2,4–6] For the experimental investigation of the phase separation behaviour, the liquid–liquid system within the cell is first dispersed and then separated while the phase separation behaviour is observed. Accordingly, based on the obtained experimental data, a model is parameterized, which is used to design the settler. Due to its simple application, low chemical consumption and computing effort, this method is well-established.^[4–7] However, a significant disadvantage of Henschke's model is the assumption of a monodisperse droplet size distribution (DSD). This assumption can lead to an inaccurate model prediction of the phase separation behaviour within a settler and thus to an under- or over-sizing of the settler.^[2] In order to increase the accuracy of the model prediction, the existing models must consider the polydispersity of the DSD. To address this challenge, several authors developed suitable models based on a polydisperse consideration of the DSD^[8,9] to describe individual phenomena during the phase separation, for example, coalescence during the sedimentation process. However, considering the initial state of the phase separation process in the settling cell was neither investigated experimentally nor model-based. The initial state occurs as soon as the mixing step of the settling experiment is completed and is characterized by the initial DSD resulting from the mixing step.^[2] Knowing the initial DSD is essential for a model-based description of the phase separation process considering polydispersity.

This work aims to describe the initial DSD in the standardized batch-settling cell, both phenomenological and model-based. For this purpose, mixing experiments are performed in the settling cell at relevant operating conditions for settling experiments. The material systems are chosen to cover the range of physical properties relevant to separation tasks in a settler. The experimental results are compared with the observations in mixing technology from the literature and explained phenomenologically. Moreover, established models from the mixing technology are applied to describe the SMD and DSD and the most suitable models are identified. The suitable models must, on the one hand, represent the

defined range of the material system's physical properties and operating conditions accurately. On the other hand, a model with a similarly low computational effort as the Henschke's method is preferred to be easily implemented in this method.

The study is organized as follows: First, the theoretical foundations of DSD in mixing processes are introduced. Second, the approach to investigating DSD on an experimental and model-based basis is described. Third, the experimental results and the model-based description of the DSD are discussed. Finally, a summary and an outlook are provided.

2 | FUNDAMENTALS

Since the batch settling cell is a stirred vessel, the theoretical foundations on stirred vessels can describe the mixing behaviour and, thus, the initial DSD in the settling cell, both phenomenological and model-based. The DSD in liquid–liquid systems results from droplet breakage and coalescence mechanisms.^[10] Several authors have reviewed experimental investigations and modelling approaches of DSD in stirred vessels.^[10–12] In addition to the stirrer and vessel geometry, the main parameters influencing droplet breakage and coalescence and, thus, the DSD are the stirrer speed and the dispersed phase fraction, referred to as hold-up in the following. Moreover, material system properties, for example, phase densities, viscosities, and interfacial tension, influence the DSD, whereby the density ratio plays a relatively minor role.^[13–20]

Besides distribution functions, the DSD is described by characteristic diameters, Sauter mean diameter (SMD) d_{32} , d_{05} , and d_{95} . The last two represent particular volume fractions of the cumulative volume distribution.^[21,22] Approaches based on mechanistic models and dimensionless numbers describing the SMD of the DSD^[16,23,24] in combination with simple correlations between the SMD and DSD^[25] are well suited to model the initial DSD in a batch settling cell. These approaches require a similarly low computational effort as Henschke's method for settler design and can be easily implemented in this method. Since no scaling is intended, but only the description of the mixing behaviour in the settling cell depending on relevant influencing parameters, these models are also sufficiently accurate.^[10,23]

The appropriate model for the SMD depends primarily on the energy spectrum range of the present turbulent flow in which the droplets are located.^[24] Moreover, it depends on the material system properties and the hold-up.^[24,26,27] Due to the broad range of material systems relevant to separation tasks in a settler, models that consider a broad range of material system properties

should be selected. Moreover, batch settling experiments are typically conducted at hold-ups of 25–50 vol.%.^[2,4–7] Assuming homogeneity of the vessel content and a dispersion located in the inertial sub-range of the energy spectrum, the model of Calabrese et al.^[26] (Equation (1)) can be applied to describe the SMD of the DSD. This model is based on an extensive experiments database and valid for hold-ups up to 0.5 vol.%, dispersed phase viscosities of 0.001–1 Pas, and interfacial tensions of 1–45 mN/m.^[18,26]

$$\frac{d_{32}}{L} = C_1(1 + 3\phi) \left[\frac{We}{1 + C_2(1 - 2.5\phi)Vi\left(\frac{d_{32}}{L}\right)^{1/3}} \right]^{-3/5}, \quad (1)$$

here, d_{32} is the SMD, L the characteristic length, typically the impeller diameter, and ϕ the hold-up. Furthermore, the Weber number We and viscosity group Vi are dimensionless expressions representing the ratio of the continuous phase inertial forces to surface forces acting on the droplet (We) and the ratio of the dispersed phase viscous forces to surface forces resisting droplet deformation (Vi).^[24] We and Vi are given by $We = \rho_c n^2 L^3 / \gamma$ and $Vi = (\rho_c / \rho_d)^{1/2} \eta_d n L / \gamma$, where n is the stirrer speed, η_d the dispersed phase viscosity, γ the interfacial tension, and ρ_c and ρ_d the continuous phase and dispersed phase densities, respectively. Both dimensionless empirical constants C_1 and C_2 are dependent on the apparatus geometry and are fitted to experimental data.

Although Equation (1) considers the hold-up influence on the SMD, Calabrese et al. proposed using Equation (1) only as a first approximation of SMD if the hold-up is higher than 0.5 vol.%.^[26] Kraume et al. have shown that a model in that form cannot accurately reflect the hold-up influence at values greater than 5 vol.%.^[15] A more accurate model that can be applied for higher hold-ups was proposed by Razzaghi and Shahraki.^[27] (Equation (2)).

$$\frac{d_{32}}{L} = C_3(1 + C_4\phi)We^{f(\phi)} \quad (2)$$

In Equation (2), C_3 and C_4 are empirical constants similar to C_1 and C_2 (Equation (1)), and $f(\phi)$ is either an empirical constant C_5 or a linear function $f(\phi) = C_6\phi + C_7$ with C_6 and C_7 as empirical constants.^[27] The studies by Kraume et al. show an almost linear correlation between $f(\phi)$ and the hold-up in the hold-up range of approximately 5–20 vol.% and an almost constant correlation in a range of approximately 20–50 vol.% for the most investigated material systems.^[15] Conversely, the investigation of Razzaghi and

Shahraki^[27] on experimental data of Desnoyer et al.^[14] shows that in dependence on the material system, the correlation between $f(\phi)$ and the hold-up can switch between almost constant and linear in a hold-up range of 5–20 vol.% and is almost linear in a hold-up range of 20–60 vol.%. However, the model proposed by Razzaghi et al. does not consider the ratio of the dispersed phase viscous forces to surface forces resisting droplet deformation.

Neither the model of Calabrese et al. nor the model of Razzaghi and Shahraki considers the influence of continuous phase viscosity on the SMD. This disregard is due to the model's derivation from the force equilibrium acting on the droplet and the assumption that the disruptive forces are purely due to the stress exerted by the continuous phase turbulence and not viscous stress.^[24] However, experimental investigations show that continuous phase viscosity significantly influences the SMD.^[13] To consider the influence of continuous phase viscosity on the SMD either the viscous sub-range of the energy spectrum must be assumed^[24] or the models must be modified by adding the viscosity ratio $(\eta_d / \eta_c)^{C_8}$, where η_c is the continuous phase viscosity and C_8 another empirical constant.^[28,29]

Describing the DSD in dependence on the SMD primarily requires knowledge about the DSD type. Typical types of DSD in stirred vessels are Gaussian, log-normal, and Weibull DSD.^[16] A method to identify the distribution type is to determine the distribution's skewness.^[30] Determining skewness based on L-moments according to Hosking^[31] is particularly suitable because this method has several advantages^[32,33] compared to other methods,^[30,34] for example, low sensitivity to outliers and low computational effort. After the skewness is determined, it can be assigned to a skewness range according to Bulmer.^[35] Based on this range, the distribution can be called approximately symmetric, and thus Gaussian, or positive skewed, and thus log-normal, or Weibull. To make a statement about the confidence of the determined skewness, confidence intervals are typically examined.^[36,37] Determining the confidence intervals using the bias-corrected percentile bootstrap approach according to Efron^[37,38] is suited for DSDs as it is most accurate with positive skewness and extensive data sets.^[36,37] Moreover, the bootstrap method can be used to determine the confidence interval of all distribution-based parameters.^[30] The consideration of distribution's skewness and the determination of its confidence intervals using the bootstrap method are standard statistical methods in medicine and finance^[39–41] and have yet to be used in the context of DSD.

If the DSD type is known, the DSD can be described using the corresponding cumulative distribution function

(CDF), as shown in Equation (3), for example, for a log-normal DSD.^[24]

$$F_v(d_i) = \frac{1}{2} \left[1 + \operatorname{erf} \left(\frac{\ln(d_i) - \mu_{\ln}}{\sigma_{\ln} \sqrt{2}} \right) \right] \quad (3)$$

In Equation (3), d_i is the droplet diameter, μ_{\ln} the mean, and σ_{\ln} the standard deviation of logarithmic values. The parameters μ_{\ln} and σ_{\ln} are fitted to the experimental data of the DSD. Moreover, by normalizing the parameters μ_{\ln} and σ_{\ln} with the SMD, the self-similarity of different DSDs can be examined.^[15,18] Since μ_{\ln} and σ_{\ln} describe logarithmic values of the mean and the standard deviation, these values cannot be used for a direct interpretation of the mean and the standard deviation. To enable a direct interpretation μ_{\ln} and σ_{\ln} are converted to μ and σ according to Equations (4) and (5).

$$\mu = \exp \left(\mu_{\ln} + \frac{\sigma_{\ln}^2}{2} \right) \quad (4)$$

$$\sigma = \sqrt{\exp(2\mu_{\ln} + \sigma_{\ln}^2)(\exp(\sigma_{\ln}^2) - 1)} \quad (5)$$

The confidence intervals of the parameters μ and σ can be determined using the bootstrap method according to Efron.^[37,38] If the parameters μ and σ of the CDF are known, they can be linked to the SMD (Equations (6) and (7)) as proposed by Schmitt et al.^[25]

$$\mu = C_9(d_{32})^{C_{10}} \quad (6)$$

$$\sigma = C_{11}(d_{32})^{C_{12}} \quad (7)$$

For the fitting of the parameters C_i , μ , and σ in Equations (1)–(3), the mean absolute percentage error (MAPE) (Equation (8)) can be used as a minimization function, where N_f is the number of fitted points, and A_i and P_i are the actual and predicted values, respectively.

$$\text{MAPE} = 100 \frac{1}{N_f} \sum_{i=1}^{N_f} \left| \frac{A_i - P_i}{A_i} \right| \quad (8)$$

3 | MATERIALS AND METHODS

First, the experimental set-up, the material systems investigated in this work, and the test plan and procedure are introduced. Second, the procedure for data analysis and the model-based description of the SMD and DSD are described.

3.1 | Experimental set-up

The mixing experiments were conducted in the automated, standardized batch-settling cell, as introduced by Sibirtsev et al.^[5] The DSD was measured using an endoscope type Sc-VR420-C22402 with a mirror and PTFE reflectors (Sopat GmbH, Berlin, DE). Further details regarding the stirrer and vessel geometry, the arrangement of the stirrers, and the position of the endoscope probe inside the settling cell can be found in the Data S1, Section S6.1.

3.2 | Material system

Two saturated biphasic systems are used in the investigation of DSD in the mixing experiments: the 2-methyltetrahydrofuran (2-MTHF)/water system with a low interfacial tension and the decane/water system with a high interfacial tension. Moreover, to investigate the influence of the viscosity on the DSD, glycerol is added in different proportions to the decane/water system. The glycerol dissolves entirely in the aqueous phase and modifies its physical properties. The addition of glycerol did not result in any discernible change in the physical properties of the organic phase. Furthermore, the ionic strength was adjusted to 50 mmol/L using sodium chloride, as detailed by Soika and Pfennig.^[42] Table 1 shows the physical properties of the saturated biphasic system. Further information on the material system and the measurement of physical properties and chemicals can be found in the Section S6.2.

3.3 | Test plan and procedure

A test plan was designed to investigate the relevant influencing parameters on the DSD, known from the literature (Section 2). The main influencing parameters are interfacial tension, phase viscosities, hold-up, and stirrer speed. The interfacial tension is varied by the choice of the material system (Section 3.2). Since glycerol is soluble only in aqueous solutions, the impact of the viscosity of the continuous phase (oil-in-water dispersion [o/w]) and the viscosity of the dispersed phase (water-in-oil dispersion [w/o]) is examined by varying the composition of the dispersed phase in the decane/water system. However, adding glycerol also influences the interfacial tension and the continuous phase density and, thus, the density ratio. The change in the density ratio plays a comparably minor role, while the change in interfacial tension is significant.^[18,19] The experiments are conducted at hold-ups of 25–50 vol.%. A lower and upper boundary limit the range of the investigated stirrer speed.

TABLE 1 Physical properties of the saturated biphasic systems at ambient temperature of 22°C.

$T = 22^{\circ}\text{C}$		Glycerol fraction wt. %	Density kg/m^3	Viscosity mPas	Interfacial tension mN/m
System 1	2-MTHF	-	862	0.61	-
	Water	0	989	1.52	2.7
System 2	Decane	-	730	0.90	-
	Water	0	998	0.97	51.5
		30	1073	2.30	44.9
		70	1180	19.10	36.0
		80	1208	48.50	33.8

The lower boundary is determined by the dispersion's homogeneity and the maximum detectable droplet size by the endoscope probe. On the one hand, both phases must be visually mixed, and on the other hand, the droplets detected with the endoscope probe must not be larger than the probe's visible range. In order to prevent the introduction of air bubbles into the dispersion, it is necessary to define the upper boundary as the point at which air is introduced as a result of the mixing process. Consequently, the minimum and maximum stirrer speeds were established based on the aforementioned criteria for each test individually. The initial stirrer speed was set at 350 and 50 min^{-1} increments were applied until the two boundaries were identified. Only experimental data between the two boundaries is considered for investigation of influences on SMD and DSD. A minimum of 450 endoscope images, corresponding to 2000–5000 droplets, were recorded at each stirrer speed to ensure a representative droplet amount.^[25,43] The test plan presented in Table 2 covers a broad range of material system's physical properties relevant to separation tasks in settler and operating conditions in settling experiments (Section 2). The notation of the test numbers and the intended study objectives of the individual tests concerning the parameter influence can be found in the Section S6.3.

3.4 | Data analysis

An automated image processing method presented by Sibirtsev et al.^[22,44,45] is used to evaluate the recorded endoscope images and to determine the experimental DSDs. Moreover, the measured DSD data is filtered before determining the SMD and the DSD type. Detailed information on data analysis can be found in Sections S6.4–S6.6.

3.4.1 | Data filtering

The DSD data is filtered to a representative DSD volume of 90 vol.%, which lies between d_{05} and d_{95} (Section S6.4).

Droplet diameters exceeding d_{95} were excluded from the analysis, as they are deemed to be comparatively inaccurate. This is due to the low number of droplets in this range, which renders them unrepresentative of the DSD.^[22,45] Moreover, droplet diameters smaller than d_{05} are removed from the analysis in order to compensate for the removal of droplet diameters larger than d_{95} . This ensures that the determination of the DSD skewness is not distorted. As a result, droplet diameters between d_{05} and d_{95} are used to determine the parameters SMD and DSD skewness and for the fitting of the CDF. The filtering of the DSD data has a negligible effect on determining DSD-based parameters, for example, the average deviation in the SMD is less than 2%. However, the filtering process effectively removes outliers, significantly enhancing the reliability of determining these parameters.

3.4.2 | Sauter mean diameter

The influence of the investigated parameters (Section 3.3) on the SMD is analyzed, and the resulting findings are compared with those from the literature (Section 2). The relative error of the determined SMD corresponds to 3% and results from the image processing method.^[22,45]

3.4.3 | Droplet size distribution type

The DSD type is identified based on the DSD skewness t_3 determined according to Hosking^[31] and assigned to a skewness range according to Bulmer.^[35] The result of the assignment identifies whether the DSD is approximately symmetric, and thus Gaussian, or positive skewed, and thus log-normal, or Weibull. The CDF fitting error introduced in Section 3.5.2 is employed to determine whether a positive skewed DSD is log-normal or Weibull based. Furthermore, the bias-corrected percentile bootstrap approach, as described by Efron, is used to ascertain the confidence intervals of the DSD skewness.^[38]

TABLE 2 Test plan.

	Glycerol fraction wt. %	Dispersion type	Hold-up vol. %	Test number
System 1	0	o/w	33	1A0F
			50	1A0H
		w/o	33	1A3F
System 2	0	o/w	25	2A0E
			33	2A0F
			40	2A0G
		w/o	25	2A3E
			33	2A3F
			40	2A3G
	30	o/w	25	2B0E
			33	2B0F
			40	2B0G
		w/o	25	2B3E
			33	2B3F
			40	2B3G
	70	o/w	25	2C0E
			33	2C0F
			40	2C0G
		w/o	25	2C3E
			33	2C3F
			40	2C3G
	80	o/w	25	2D0E
			33	2D0F
			40	2D0G
		w/o	25	2D3E
			33	2D3F
			40	2D3G

3.5 | Model-based description

This study uses correlations from the literature (Section 2) to model the SMD and the DSD. Furthermore, a model-based connection between the SMD and DSD is investigated. Section S6.7 summarizes all investigated models in this work. All parameter fittings are performed with the *fmincon* solver of MATLAB® using the MAPE (Equation (8)) as minimization function and fitting error. Parameter settings of the *fmincon* solver can be found in the Section S6.8.

3.5.1 | Sauter mean diameter

A comparison is made between different correlations in order to model the SMD, including Equations (1) and (2) (Table S4). Moreover, Equation (9) is tested, which is a

combination of Equations (1) and (2). Equation (9) allows the consideration of the dispersed phase viscous forces to surface forces resisting droplet deformation according to Equation (1) and the higher hold-ups according to Equation (2). Moreover, Equation (9) considers the viscosity ratio $(\eta_d/\eta_c)^{C_{14}}$.

$$\frac{d_{32}}{L} = C_{13} \left(\frac{\eta_d}{\eta_c} \right)^{C_{14}} (1 + 3\phi) \left[\frac{We}{1 + C_{15}(1 - 2.5\phi) Vi \left(\frac{d_{32}}{L} \right)^{1/3}} \right]^{f(\phi)} \quad (9)$$

Analogous to Equation (2), a test is conducted to ascertain whether $f(\phi)$ is an empirical constant C_{16} (Equation (9a), Table S4) or a linear function $f(\phi) = C_{17}\phi + C_{18}$ (Equation (9b), Table S4). Moreover, a simplified version of Equation (9) is also tested, which

excludes the viscosity ratio term (Equation (9c), Table S4) to test whether the consideration of the continuous phase viscosity has a significant influence on the model accuracy.

For all investigated correlations, the length L is set to $L = N_s D$, where $N_s = 7$ is the number of stirrers, and $D = 39$ mm is the stirrer diameter (Section S6.1).

3.5.2 | Cumulative distribution function

Depending on the DSD skewness (Section 3.4), Gaussian, log-normal, or Weibull CDFs are fitted to the experimental DSD data. The log-normal and Weibull CDFs were fitted to positive skewed DSDs, and the most suitable CDF was selected based on the MAPEs of these fits. Moreover, μ_{\ln} and σ_{\ln} was converted to μ and σ according to Equations (4) and (5) to enable a direct interpretation of the log-normal CDF parameters mean and standard deviation. In addition, the droplet diameters of the DSDs with the SMD were normalized to determine the CDF's normalized means and standard deviations. Based on the normalized values, the self-similarity of the measured DSDs was examined. Finally, the CDF parameters μ and σ were correlated with the SMD according to Equations (6) and (7).

4 | RESULTS AND DISCUSSION

This chapter shows the results of experimental and model-based investigations on the SMD and DSD. The experimental results are discussed phenomenologically and compared with the findings from the literature. Moreover, different correlations are compared to model the SMD and DSD.

The individual test results on the SMD, the DSD skewness, and CDF parameters mean μ , and standard deviation σ are shown in this chapter as examples. All test results of this study can be found in the Section S6.9.

In advance, the DSD measurement of the decane/water system did not lead to valid results due to the poor droplet detection performance for the following constellations: complete test series of the w/o dispersion and partial tests with o/w dispersion at glycerol fractions of 30 and 70 wt.%. Therefore, the results of these measurements are not considered in the following.

4.1 | Sauter mean diameter

4.1.1 | Experimental investigation

Figure 1 shows the SMD of the 2-MTHF/water system and decane/water system at a glycerol fraction of 0 wt.%

in dependence on the stirrer speed and the hold-up. For all conducted tests (Figures 1 and S12–S14), the SMD decreases with increased stirrer speed. Increasing stirrer speed increases the energy dissipation rate and, thus, the droplet breakage rates.^[14,16] Moreover, for all conducted tests, the SMD increases with the increase in hold-up. Increasing hold-up increases the droplet collision rates, which benefits the coalescence phenomenon.^[13–15] The phase inversion from w/o to o/w for the 2-MTHF/water system decreases the SMD. Due to this phase inversion, the dispersed phase viscosity is decreased, which benefits the breakage phenomenon.^[15,18] Comparing both material systems at a hold-up of 33 vol.%, the SMD of the decane/water system is higher than the SMD of the 2-MTHF/water system at the same stirrer speeds. The significant effect that leads to this result is the lower interfacial tension of the 2-MTHF/water system. A lower interfacial tension results in higher breakage rates and thus lower SMD.^[18]

Figure 2 shows the SMD of the decane/water system at a hold-up of 25 vol.% in dependence on the stirrer speed and glycerol fraction. In most performed tests (Figures 2 and S15, S16), the increase in glycerol fraction decreases the SMD. Due to the increase in glycerol fraction, the interfacial tension decreases, whereby the continuous phase viscosity and the density ratio of the continuous phase to the dispersed phase increase. The change in the density ratio plays a comparably minor role, while the change in interfacial tension and continuous phase viscosity plays a significant role.^[13,18,19] The decrease in interfacial tension benefits the breakage phenomenon.^[18] In addition, the increase in continuous phase viscosity inhibits the film drainage during the coalescence process and thus the coalescence phenomenon.^[13] Since both effects decrease the SMD, a posterior differentiation between them is not possible within the scope of this investigation. One method for identifying the dominant effect is to examine the performance of the SMD model, as discussed in Section 4.1.2. If a model that considers the interfacial tension but not the continuous phase viscosity provides similarly accurate results as a model that considers both influencing parameters, it can be assumed that the continuous phase viscosity is insignificant.

A notable exception to the typical SMD behaviour in dependence on the glycerol fraction is observed at a hold-up of 25 vol.% (Figure 2). At this hold-up, the SMD initially increases with the glycerol fraction from 0 to 30 wt.%, and then decreases from 30 to 80 wt.%. This behaviour, as explained by Stamatoudis and Tavlarides in their investigations of specific material systems, hold-ups, and stirrer speeds, is attributed to the increase in continuous phase viscosity. The increase in continuous phase viscosity inhibits both the breakage and coalescence phenomena, with the dominant inhibition depending on the material system, hold-up, and stirrer speed. Importantly, in the investigations of Stamatoudis and Tavlarides, the change

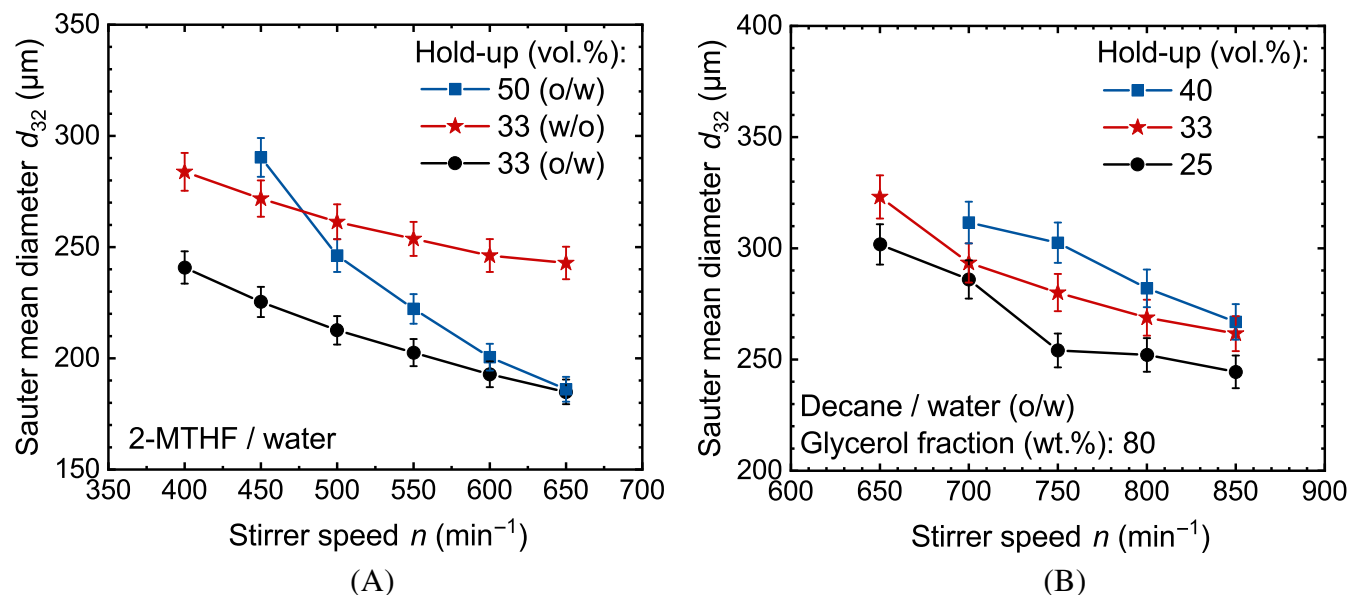


FIGURE 1 Sauter mean diameter in dependence of the stirrer speed and the hold-up for the systems: (A) 2-methyltetrahydrofuran (2-MTHF)/water and (B) decane/water at glycerol fraction of 0 wt.%.

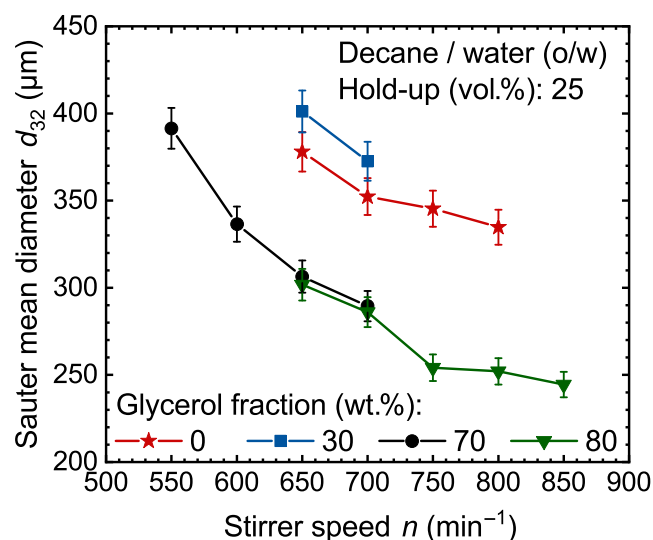


FIGURE 2 Sauter mean diameter of the decane/water systems in dependence on the glycerol fraction at hold-up of 25 vol.%.

in glycerol fraction significantly influenced the continuous phase viscosity while the interfacial tension remained relatively constant.^[13]

4.1.2 | Model-based description

The SMD correlations considered in this work (Table S4) are fitted to the measured SMD data. The MAPEs of the fits are compared to identify the most accurate correlation. The most accurate performance shows Equation (9b) with

a MAPE of 3.6% (Table S4). Compared to other models, Equation (9b) considers the most influencing parameters on the SMD. However, Equation (9b) also has the most number of fitting parameters, which is five.

$$\frac{d_{32}}{L} = 0.0026 \left(\frac{\eta_d}{\eta_c} \right)^{0.032} (1 + 3\phi) \left[\frac{We}{1 + 0.03(1 - 2.5\phi) Vi \left(\frac{d_{32}}{L} \right)^{1/3}} \right]^{0.11\phi + 0.22} \quad (9b)$$

The most inaccurate performance shows Equation (1) with a MAPE of 18.7% (Table S4). In Equation (1), the correlation's exponent $f(\phi)$ is not fitted to experimental data but set to a constant value of $-3/5$. Thus, we expect that using a constant exponent of $-3/5$ is insufficient to consider the hold-up influence on the SMD for hold-ups between 25 and 50 vol.%. Other researchers have shown similar findings.^[15,27]

In the next step, the MAPEs of Equations (9a) and (9b), which are 5.4% and 3.6%, respectively, are compared. Moreover, the MAPEs of Equation (2), which are 5.5% and 5.3%, respectively, are compared. The comparisons show that regarding hold-up influence on the SMD in the range of 25–50 vol.%, it makes only a small difference whether the exponent $f(\phi)$ is a linear function or an empirical constant fitted to experimental data. Although Razzaghi and Shahraki^[27] have shown that the exponent $f(\phi)$ is a linear function of the hold-up in a hold-up range of 25–50 vol.%, the investigation of Kraume et al.^[15] shows that in this hold-up range, $f(\phi)$ is almost constant, which is more consistent with the results of our work.

However, since our results partly contradict the findings from the literature, further investigations of the hold-up influence on the SMD for other material systems should be carried out in future work.

Even since Equation (2) do not consider the ratio of the dispersed phase viscous forces to surface forces resisting droplet deformation, their performance is comparable with the accurate performance of Equations (9a) and (9b). As the complete test series investigating the w/o dispersion of the decane/water system was excluded in this work, only a limited amount of data was available in which the dispersed phase viscosity varied. Moreover, based on an extensive database of experiments, Wang and Calabrese showed that the dispersed phase viscosity significantly influences the SMD.^[18] Therefore, it is assumed that the influence of dispersed phase viscosity is not noticeable in our investigations and the accurate performance of Equation (2) results from this lack of data. This assumption should be validated in future work through targeted investigations of the influence of the dispersed phase viscosity.

Furthermore, the MAPEs of Equations (9a) and (9c), which are 5.4% and 6.6%, respectively, hardly differ. The difference between Equations (9a) and (9c) is the consideration of the viscosity ratio in Equation (9a) and, thus, especially the consideration of the continuous phase viscosity. As discussed in Section 4.2.1, comparing the MAPEs of Equations (9a) and (9c), therefore, enables us to identify whether the decrease in interfacial tension or the increase in continuous phase viscosity is primarily responsible for the decrease in the SMD due to a change in glycerol fraction. Since the MAPEs of Equations (9a) and (9c) hardly differ, we assume that the continuous phase viscosity plays a minor role in our investigations. Since the increase in continuous phase viscosity inhibits both the breakage and coalescence phenomena,^[13] we assume that the opposing influences of these phenomena on the SMD neutralize each other, resulting in a constant SMD. However, since Stamatoudis and Tavlarides^[13] have shown that continuous phase viscosity can significantly influence the SMD, this effect should be investigated using suitable material systems in future work.

Based on our findings and the literature findings, we assume that choosing the appropriate SMD model depends on the range of hold-up and physical properties to be represented. In a range of 25–40 vol.%, it is necessary to consider the hold-up influence on the SMD by fitting the correlation's exponent $f(\phi)$ to experimental data. If the influence of dispersed phase viscosity on the SMD becomes significant, considering the ratio of the dispersed phase viscous forces to surface forces resisting droplet deformation (Vi) is necessary. Moreover, if the continuous phase viscosity significantly influences

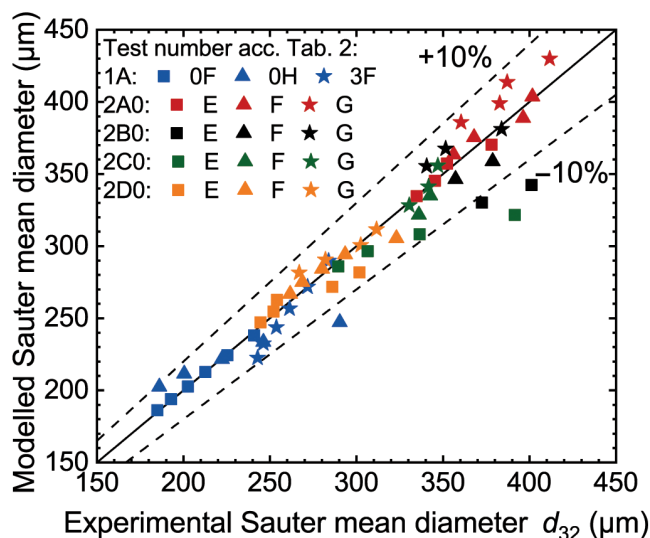


FIGURE 3 Parity plot of the Sauter mean diameter (SMD) modelled according to Equation (9b) against the experimentally determined SMD, mean absolute percentage error corresponds to 5.2%, over 93% of the data falls within an interval of $\pm 10\%$. Test numbers according to Table 2.

the SMD, the correlation should consider the viscosity ratio (η_a/η_c).

Figure 3 presents the parity plot of the SMD modelled according to Equation (9b) against the experimentally determined SMD, showcasing the accurate fit of Equation (9b). Notably, over 93% of the data falls within an interval of $\pm 10\%$ (Table S4), indicating a high level of accuracy. Furthermore, the SMD prediction is consistently accurate across the entire considered SMD range, with no specific areas showing a tendency to be under- or overestimated. All parity plots of the correlations considered in this work can be found in Section S6.10.

4.2 | Droplet size distribution

4.2.1 | Experimental investigation

Figure 4 shows exemplary CDF curves for the 2-MTHF/water and decane/water material systems at the same hold-up and stirrer speed. Comparing the CDFs of both systems, it is qualitatively recognizable that the CDF of the 2-MTHF/water system results from a DSD with smaller droplet diameters and a more symmetrical and narrow shape. However, the DSD skewness and the CDF's mean and standard deviation must be considered in detail to quantify the DSD's shape.

Figure 5 shows the DSD skewness of the 2-MTHF/water system and decane/water system at glycerol fraction of 80 wt.% in dependence on the stirrer speed and the

hold-up, highlighting the skewness ranges according to Bulmer.^[35] The only DSDs, which are approximately symmetric, are those of the 2-MTHF/water system at a hold-up of 33 vol.%, independent of the dispersion type (o/w or w/o) (Figure 5A). DSDs of the 2-MTHF/water system at a hold-up of 50 vol.% (Figure 5A) and the decane/water system at a glycerol fraction of 80 wt.% and higher rotation speeds (Figure 5B) are moderately skewed. DSDs of the decane/water system at glycerol fractions between 0 and

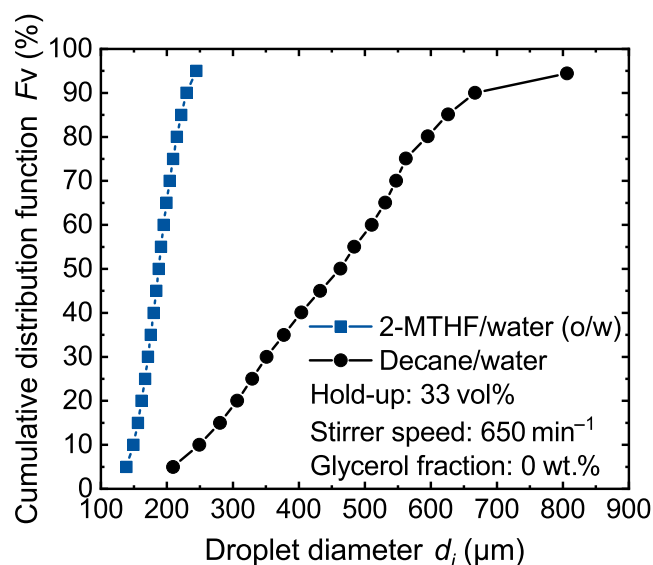
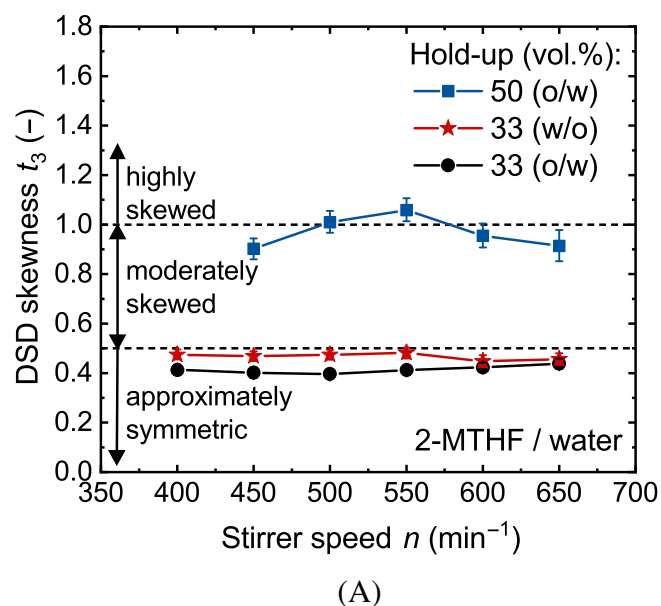


FIGURE 4 Exemplary cumulative distribution function curves for the 2-methyltetrahydrofuran (2-MTHF) and decane/water systems.



70 wt.% (Figures S17–S19) and at a glycerol fraction of 80 wt.% and low rotation speeds (Figure 5B) are highly skewed.

The skewness of the approximately symmetric DSD data is very close to the limit of moderately skewed DSD. For simplicity, this data is considered skewed, and thus, the Gaussian distribution is disregarded in further analysis. The low difference in the MAPE for the approximately symmetric DSD data, which is 2% for the Gaussian CDF and 4% for the log-normal CDF, justifies this simplification. Regarding the whole DSD data, the Weibull distribution is also excluded from further analysis since the MAPE of the Weibull CDF is 10% in contrast to the log-normal CDF, which is 5%. Therefore, a log-normal CDF represents all of this work's DSDs.

The DSD skewness and the CDF parameters mean μ and standard deviation σ are analyzed to investigate further the DSD behaviour in dependence on the influencing parameters. The mean μ behaves similarly to the SMD (Section 4.1.1). Thus, the behaviour of μ is not illustrated explicitly at this point and can be found in the Section S6.9.3.

Increasing the stirrer speed, the glycerol fraction, or decreasing the hold-up decreases the mean for all conducted tests (Figures S22–S29). The DSD skewness remains almost constant for the 2-MTHF/water system (Figure 5A) and decreases for the decane/water system (Figure 5B) in dependence on the stirrer speed.

Figure 6 presents the standard deviation σ of the 2-MTHF/water system and decane/water system at glycerol fraction of 80 wt.% in dependence on the stirrer speed and

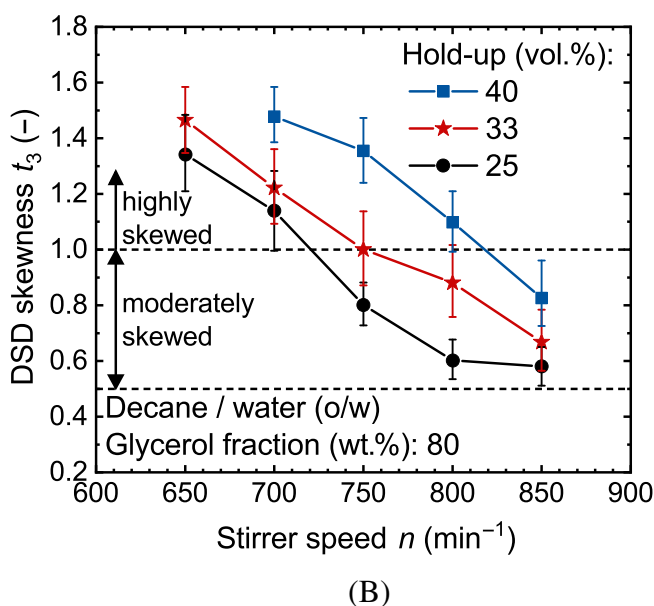


FIGURE 5 Droplet size distribution skewness in dependence of the stirrer speed and the hold-up for the systems: (A) 2-methyltetrahydrofuran (2-MTHF)/water and (B) decane/water at glycerol fraction of 0 wt.%.

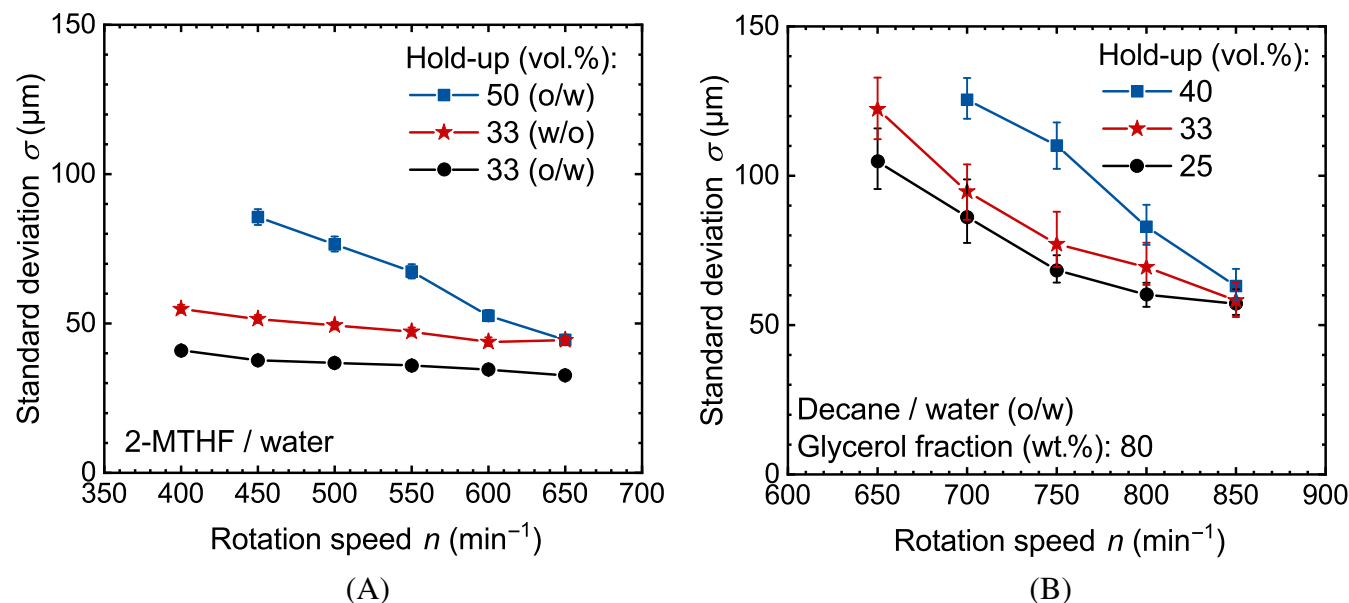


FIGURE 6 Cumulative distribution function Standard deviation in dependence of the stirrer speed and the hold-up for the systems: (A) 2-methyltetrahydrofuran (2-MTHF)/water and (B) decane/water at glycerol fraction of 80 wt.%.

the hold-up. Increasing the stirrer speed decreases the standard deviation for all conducted tests (Figures 6 and S30–S32) except the tests with the 2-MTHF/water system at a hold-up of 33 vol.% (Figure 6A). Here, σ remains comparatively constant independent of the dispersion type (o/w or w/o). Both the DSD skewness (Figures 5 and S17–S19) and the standard deviation (Figures 6 and S30–S32) tend to increase with an increase in hold-up. A single exception is observed for the decane/water system at a glycerol fraction of 0 wt.%, where the skewness decreases with an increase in hold-up.

Figure 7 shows the DSD skewness and the standard deviation of the decane/water system at a hold-up of 33 wt.% in dependence on the stirrer speed and the glycerol fraction. Both the DSD skewness (Figures 7A and S20, S21) and the standard deviation (Figures 7B and S33, S34) tend to decrease with an increase in glycerol fraction. As discussed in Section 4.1, the change in interfacial tension due to a change in glycerol fraction primarily affects the DSD. Therefore, increasing the decane/water system's interfacial tension increases the DSD skewness and CDF standard deviation.

In summary, the tests show that the DSD shape remains almost constant, increasing the stirrer speed for material systems with lower interfacial tensions and hold-ups (Figures 5A and 6A). The DSD only shifts to smaller diameters, observed by a decrease in the CDF mean (Figure S22). For material systems with lower interfacial tensions but higher hold-ups, the DSD not only shifts to smaller diameters (Figure S22) but the DSD shape becomes narrower due to an increase in the stirrer

speed, which is observed due to a decrease in the CDF standard deviation (Figure 6A). However, the systems' symmetry does not change (Figure 5A). For material systems with higher interfacial tension, the DSD shape becomes narrower (Figures 6B and S30–S32) and more symmetrical (Figures 5B and S17–S19) when increasing the stirrer speed, while the DSD shifts to smaller diameters (Figures S23–S26). Moreover, increasing the hold-up makes the DSD shape broader and more asymmetrical, independent of the material system.

Comparing these results with the investigation of Wang and Calabrese^[18] and Zerfa and Brooks^[17] confirms the observations of this work. The balance between droplet breakage and coalescence determines the shape of the DSD.^[15] Material systems with low interfacial tension and hold-up have comparably high breakage rates and low coalescence rates,^[15] which can result in a narrow and symmetrical DSD shape.^[17,18] Increasing the stirrer speed and, thus, the breakage rate does not significantly affect these systems' DSD shape. Material systems with high interfacial tension or hold-up have comparably low breakage rates and high coalescence rates,^[15] which can result in a broad and asymmetrical DSD shape. An increase in the breakage rate significantly influences these systems' DSD shape.

The investigation of self-similarity showed that only the o/w and w/o dispersion of the 2-MTHF/water system at a hold-up of 33 vol.% is self-similar with an accuracy comparable to that in the literature.^[15,18] At a hold-up of 50 vol.%, the 2-MTHF/water system deviates from this self-similarity. No self-similarity can be

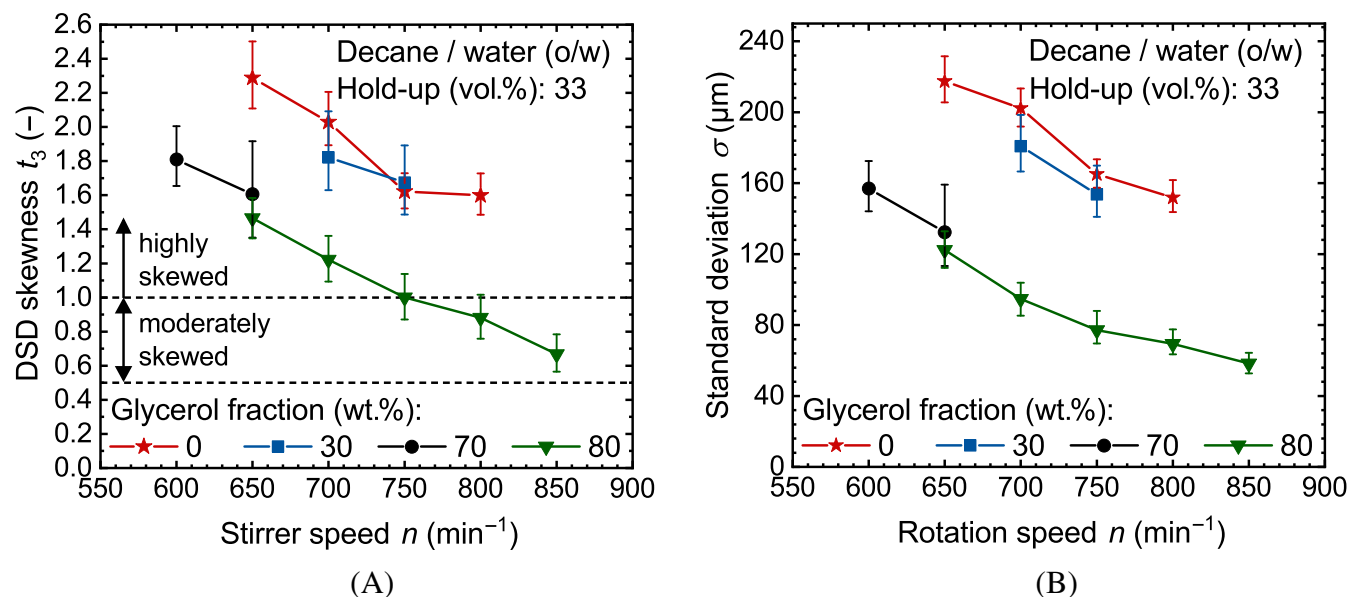


FIGURE 7 Droplet size distribution (DSD) parameters of the decane/water system in dependence on the stirrer speed and glycerol fraction: (A) DSD skewness and (B) standard deviation of the cumulative distribution function.

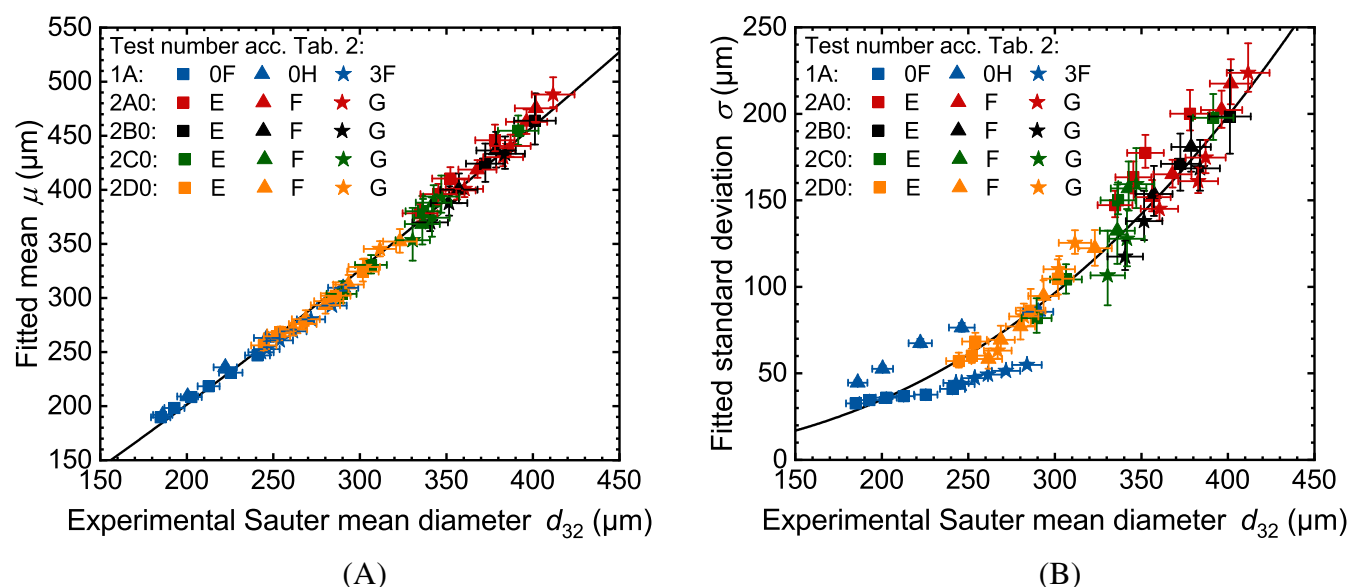


FIGURE 8 Correlation between the Sauter mean diameter and the (A) mean and (B) standard deviation of the cumulative distribution function. Test numbers according to Table 2.

identified for the decane/water system or between both material systems.

4.2.2 | Model-based description

Figure 8 shows the CDF's mean and standard deviation in dependence on the experimentally determined SMD. Both parameters increase with an increase in SMD and correlate with the SMD according to Equations (10)

and (11). For all performed tests, correlating the mean by Equation (10) results in an accurate prediction. Correlating the standard deviation by Equation (11) is accurate for the decane/water system but less accurate for the 2-MTHF/water system, especially at a hold-up of 33 vol. %. One possible explanation for this result is that our simplification considering this data to be skewed is an inaccurate assumption. Future investigations with material systems and operating conditions in this area should be performed to check our simplification. However, testing

the MAPE between the fitted CDFs and CDFs calculated with the mean and standard deviation according to Equations (10) and (11) results in a MAPE of 11.4%. Thus, the DSD can, on average, be determined accurately based on Equations (10) and (11).

$$\mu = 0.374(d_{32})^{1.19} \quad (10)$$

$$\sigma = 5.73 \cdot 10^{-5}(d_{32})^{2.51} \quad (11)$$

The interpolation capability of the determined models is valid approximately between hold-ups of 25–50 vol.%, interfacial tensions of 3–52 mN/m, continuous phase densities and viscosities of 862–1208 kg/m³ and 1–49 mPas, respectively, and dispersed phase densities and viscosities of 730–989 kg/m³ and 0.6–1.5 mPas, respectively.

5 | CONCLUSION

The experimental investigation shows that the DSD data corresponds to a log-normal distribution. Increasing the stirrer speed decreases the SMD for all investigations. The DSD shape becomes narrower and more symmetrical with increased stirrer speed for material systems with high interfacial tension or hold-up and remains almost constant for systems with low interfacial tension and hold-up. Moreover, with an increase in hold-up, the SMD increases, and the DSD shape becomes broader and more asymmetrical. Furthermore, material systems with lower interfacial tensions result in lower SMDs and narrower and more symmetrical DSD shapes. The continuous phase viscosity plays a minor role.

The model-based investigation shows that a Weber number correlation (Equation (9c)) describes the SMD with a MAPE of 3.6%. Fitting the log-normal CDF (Equation (3)) to the experimental DSD data results in a MAPE of 5%. Moreover, correlations between the CDF's mean (Equation (10)) and standard deviation (Equation (11)) and the SMD are identified. Comparing the fitted CDFs with CDFs determined by these correlations results in a MAPE of 11.4%.

The results of this work provide helpful insights into the mixing process in a standardized batch-settling cell and offer valuable information about the initial DSD of the batch-settling experiment. The resulting SMD and DSD models form a solid foundation for modelling phase separation behaviour in the batch-settling cell considering polydispersity.

The SMD and DSD models presented in this work will be further used to describe the sedimentation and coalescence processes considering polydispersity. Furthermore,

there is potential for the SMD and DSD models to be expanded through experimental investigation of the DSD of dispersions with higher dispersed phase viscosity. In addition, investigating dispersions that are significantly influenced by the continuous phase viscosity could increase the reliability of the presented models.

AUTHOR CONTRIBUTIONS

Stepan Sibirtsev: Conceptualization; methodology; visualization; writing – original draft. **Lukas Thiel:** Writing – review and editing. **Song Zhai:** Writing – review and editing. **Yutang Toni Cai:** Investigation. **Louis Recke:** Investigation. **Andreas Jupke:** Supervision.

FUNDING INFORMATION

This work was financially supported by the Deutsche Forschungsgemeinschaft (DFG, German Research Foundation) within the framework of the priority program ‘SPP 2331: Machine Learning in Chemical Engineering’, project number 466656378.

CONFLICT OF INTEREST STATEMENT

The authors declare no potential conflict of interests.

PEER REVIEW

The peer review history for this article is available at <https://www.webofscience.com/api/gateway/wos/peer-view/10.1002/cjce.25563>.

DATA AVAILABILITY STATEMENT

The data that supports the findings of this study are available in the supplementary material of this article.

ORCID

Stepan Sibirtsev  <https://orcid.org/0000-0002-2123-4776>

REFERENCES

- [1] J. C. Godfrey, M. J. Slater, *Liquid-Liquid Extraction Equipment*, Wiley, New York **1994**.
- [2] M. Henschke, *Dimensionierung liegender Flüssig-flüssig-Abscheider anhand diskontinuierlicher Absetzversuche*, VDI Verlag, Düsseldorf **1995**.
- [3] M. Henschke, *Chem. Eng. J.* **2002**, 85, 369.
- [4] J. Steinhoff, E. Charlafti, D. Leleu, L. Reinecke, H. Franken, K. Becker, M. Kalem, M. Sixt, M. Braß, D. Borchardt, W. Bäcker, M. Wegener, S. Maaß, M. Weber, T. Acher, C. Matten, A. Pfennig, M. Kraume, H.-J. Bart, *Chem. Ing. Tech.* **2021**, 93, 1152.
- [5] S. Sibirtsev, C. B. Göbel, A. Jupke, *Chem. Ing. Tech.* **2019**, 91, 1787.
- [6] T. Frising, C. Noik, C. Dalmazzone, *J. Dispersion Sci. Technol.* **2006**, 27, 1035.
- [7] N. Kopriwa, A. Pfennig, *Solvent Extr. Ion Exch.* **2016**, 34, 622.
- [8] P. Chuttrakul, A. Pfennig, in *MSVT*, Vienna University of Technology (TU Wien) Vienna **2014**, pp. 64–67.

- [9] D. Leleu, A. Pfennig, *Chem. Eng. Technol.* **2019**, 42, 1404.
- [10] A. R. Ghotli, A. A. A. Raman, S. Ibrahim, S. Baroutian, *Chem. Eng. Commun.* **2013**, 200, 595.
- [11] R. Farzad, S. Schneiderbauer, in *SINTEF Proceedings*, SINTEF Academic Press, Trondheim, Norway **2017**, pp. 295–300.
- [12] N. K. Nere, A. W. Patwardhan, J. B. Joshi, *Ind. Eng. Chem. Res.* **2003**, 42, 2661.
- [13] M. Stamatoudis, L. L. Tavlarides, *Ind. Eng. Chem. Process. Des. Dev.* **1985**, 24, 1175.
- [14] C. Desnoyer, O. Masbernat, C. Gourdon, *Chem. Eng. Sci.* **2003**, 58, 1353.
- [15] M. Kraume, A. Gäbler, K. Schulze, *Chem. Eng. Technol.* **2004**, 27, 330.
- [16] P. A. Mahakal, H. T. Rangwala, A. W. Patwardhan, *Chem. Eng. Res. Des.* **2023**, 193, 843.
- [17] M. Zerfa, B. W. Brooks, *Chem. Eng. Sci.* **1996**, 51, 3223.
- [18] C. Y. Wang, R. V. Calabrese, *AIChE J.* **1986**, 32, 667.
- [19] O. Krzeczek, T. Trummler, E. Trautner, M. Klein, *Energies* **2023**, 16, 3160.
- [20] S. Ye, L. Hohl, E. Charlafti, Z. Jin, M. Kraume, *Chem. Eng. Sci.* **2023**, 274, 118676.
- [21] P. J. Kwakernaak, W. M. G. T. van den Broek, P. K. Currie, in *SPE Prod. Oper. Symp. Proc.*, SPE, Oklahoma City, OK **2007**, pp. SPE-106693-MS.
- [22] S. Sibirtsev, S. Zhai, M. Neufang, J. Seiler, A. Jupke, *Chem. Eng. J.* **2023**, 473, 144826.
- [23] J. Zhang, S. Xu, W. Li, *Chem. Eng. Process.* **2012**, 57–58, 25.
- [24] A. P. Gustavo, in *Effect of Surfactants on Drop Size Distributions in a Batch, Rotor-Stator Mixer*, ProQuest Information and Learning Company, Ann Arbor, MI **2005**.
- [25] P. Schmitt, S. Sibirtsev, M. W. Hlawitschka, R. Styn, A. Jupke, H.-J. Bart, *Chem. Ing. Tech.* **2021**, 93, 129.
- [26] R. V. Calabrese, C. Y. Wang, N. P. Bryner, *AIChE J.* **1986**, 32, 677.
- [27] K. Razzaghi, F. Shahraki, *Chem. Eng. Res. Des.* **2010**, 88, 803.
- [28] S. Hall, M. Cooke, A. El-Hamouz, A. J. Kowalski, *Chem. Eng. Sci.* **2011**, 66, 2068.
- [29] M. Nishikawa, F. Mori, S. Fujieda, *J. Chem. Eng. Jpn.* **1987**, 20, 82.
- [30] R. Shanmugam, R. Chattamvelli, *Statistics for Scientists and Engineers*, John Wiley & Sons Inc., Hoboken, NJ **2015**.
- [31] J. R. M. Hosking, *J. R. Stat. Soc.* **1990**, 52, 105.
- [32] P. Royston, *Stat. Med.* **1992**, 11, 333.
- [33] A. Bastianin, *Appl. Econ.* **2020**, 52, 637.
- [34] G. Brys, M. Hubert, A. Struyf, *Developments in Robust Statistics*, Physica-Verlag HD, Heidelberg **2003**, p. 98.
- [35] M. G. Bulmer, *Principles of Statistics*, Dover Publications, New York **1979**.
- [36] T. P. Hettmansperger, J. W. McKean, *Robust Nonparametric Statistical Methods*, CRC Press, Boca Raton, FL **2011**.
- [37] S. Perez-Meloand, B. M. G. Kibria, *Thailand Stat.* **2016**, 14, 93.
- [38] B. Efron, *J. Am. Stat. Assoc.* **1987**, 82, 171.
- [39] S. T. Mennemeyer, L. P. Cyr, *J. Health Econ.* **1997**, 16, 741.
- [40] J. Shi, D. Luo, X. Wan, Y. Liu, J. Liu, Z. Bian, T. Tong, *Stat. Methods Med. Res.* **2023**, 32, 1338.
- [41] C. Adcock, M. Eling, N. Loperfido, *Eur. J. Finance* **2015**, 21, 1253.
- [42] M. Soika, A. Pfennig, *Chem. Ing. Tech.* **2005**, 77, 905.
- [43] P. Schmitt, M. W. Hlawitschka, H.-J. Bart, *Chem. Ing. Tech.* **2020**, 92, 589.
- [44] S. Sibirtsev, S. Zhai, M. Neufang, J. Seiler, A. Jupke, in *Proc. Int. Solvent Extract. Conf.*, Gothenburg, Sweden, 2023, pp. 133–139.
- [45] S. Sibirtsev, S. Zhai, M. Neufang, J. Seiler, A. Jupke, *Chem. Eng. Res. Des.* **2023**, 202, 161.

SUPPORTING INFORMATION

Additional supporting information can be found online in the Supporting Information section at the end of this article.

How to cite this article: S. Sibirtsev, L. Thiel, S. Zhai, Y. T. Cai, L. Recke, A. Jupke, *Can. J. Chem. Eng.* **2024**, 1. <https://doi.org/10.1002/cjce.25563>